Rapid Communications

Angle dependence of H_{c2} with a crossover between the orbital and paramagnetic limits

Hideki Matsuoka,[1] Masaki Nakano,[1,2,*] Takashi Shitaokoshi,[1,3] Takumi Ouchi ,[4] Yue Wang,[1] Yuta Kashiwabara,[1]
Satoshi Yoshida,[1] Kyoko Ishizaka,[1,2] Masashi Kawasaki,[1,2] Yoshimitsu Kohama,[1,3]
Tsutomu Nojima ,[4] and Yoshihiro Iwasa[1,2]

[1]*Department of Applied Physics, The University of Tokyo, Tokyo 113-8656, Japan*
[2]*Quantum-Phase Electronics Center, The University of Tokyo, Tokyo 113-8656, Japan
and RIKEN Center for Emergent Matter Science (CEMS), Wako 351-0198, Japan*
[3]*The Institute for Solid State Physics, The University of Tokyo, Kashiwa 277-8581, Japan*
[4]*Institute for Materials Research, Tohoku University, Sendai 980-8577, Japan*

A pair-breaking mechanism of a superconductor under magnetic fields, namely, the origin of the upper critical field H_{c2}, can be categorized into the orbital effect and the paramagnetic effect, which have been separately discussed so far because the physical pictures are totally different. Here we propose a model that unifies these two origins into one formalism with a generalized physical picture. The obtained formula well describes the experimental results on the angle dependence of H_{c2} in a recently developed noncentrosymmetric superconductor, two-dimensional (2D) NbSe$_2$, providing essential information on the spin states of Cooper pairs in 2D NbSe$_2$. The proposed model is widely applicable to all superconductors, offering a powerful approach for comprehensive understanding of the origin of H_{c2}.

Superconductivity is usually suppressed by application of external magnetic fields above the upper critical field H_{c2}. The origins of H_{c2} are classified into two pair-breaking effects, the orbital effect and the paramagnetic effect. In the limit of the strong orbital effect (the orbital limit), the kinetic energy loss due to the magnetic-field-driven cyclotron motion of electrons causes suppression of superconductivity by forming the vortices or Meissner current. In the paramagnetic limit, on the other hand, superconductivity is suppressed by the energy gain of the spin-aligned paramagnetic state, which exceeds the gain of the condensation energy of the Cooper pairs. Within the framework of the Bardeen-Cooper-Schrieffer (BCS) theory, this paramagnetic limit is called the Pauli-paramagnetic limit and is set to be $H_P = \frac{\Delta_0}{\sqrt{2}\mu_B}$, where Δ_0 is the superconducting (SC) gap and μ_B the Bohr magneton. In a real system, however, the paramagnetic limit is sometimes enhanced above H_P, and such enhanced paramagnetic limit often provides essential information on the mechanism of superconductivity as well as its pairing symmetry [1,2].

One famous example that shows the enhanced paramagnetic limit is the CeCoIn$_5$-based Kondo superlattice, one of the noncentrosymmetric heavy Fermion systems [3–6]. The orbital effect in this system is largely suppressed owing to the small coherence length originating from the large effective

mass and, therefore, the contribution from the paramagnetic effect to H_{c2} becomes dominant in particular at low enough temperature. There, H_{c2} was found to be enhanced due to Rashba-type spin-orbit interaction (SOI) arising from broken out-of-plane space inversion symmetry. Another representative system is a recently developed noncentrosymmetric 2D Ising superconductor [7–11], where the orbital effect is totally quenched for the parallel magnetic fields because of the geometrical confinement. Consequently, H_{c2} with parallel magnetic fields ($H_{c2\parallel}$) is purely determined by the paramagnetic effect, which turned out to be dramatically enhanced due to Zeeman-type SOI originating from broken in-plane inversion symmetry, providing fundamental insights into the unique pairing mechanism termed Ising pairing [7,12]. In this system, however, H_{c2} with perpendicular magnetic fields ($H_{c2\perp}$) is limited by the orbital effect due to the large in-plane coherence length and, therefore, the dominant mechanism that limits H_{c2} should vary when the magnetic fields are rotated from the parallel to the perpendicular directions.

In this study, we focus on the angle dependence of H_{c2} in a 2D Ising superconductor. According to the Ginzburg-Landau (GL) theory, $H_{c2}(\theta)$ is generally described by either Eqs. (1) or (2):

$$\left| \frac{H_{c2}(\theta)\cos\theta}{H_{c2\perp}} \right| + \left[\frac{H_{c2}(\theta)\sin\theta}{H_{c2\parallel}} \right]^2 = 1, \qquad (1)$$

$$\left[\frac{H_{c2}(\theta)\cos\theta}{H_{c2\perp}} \right]^2 + \left[\frac{H_{c2}(\theta)\sin\theta}{H_{c2\parallel}} \right]^2 = 1. \qquad (2)$$

Equation (1) is well known as the 2D Tinkham's formula, which describes $H_{c2}(\theta)$ of 2D systems (a system satisfying the

---

*nakano@ap.t.u-tokyo.ac.jp
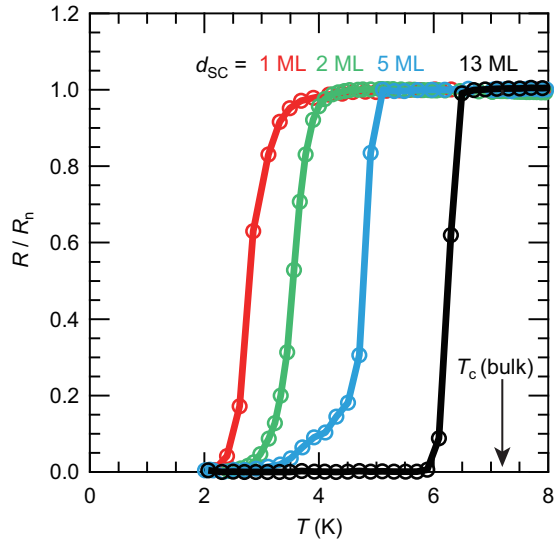
FIG. 1. The longitudinal resistance (R) versus temperature (T) curves of the MBE-grown NbSe$_2$ epitaxial thin films down to the monolayer limit. R is normalized by the normal state resistance (R_n) at $T = 8$ K. T_c defined as the temperature at $R/R_n = 0.5$ was 6.2, 4.8, 3.6, and 2.8 K for the 13-, 5-, 2-, and 1-ML-thick films, respectively. T_c of the NbSe$_2$ bulk single crystal is indicated by an arrow [23].

condition that the out-of-plane coherence length is larger than the SC thickness d_{SC}), providing the cusplike behavior around the parallel magnetic fields, as widely observed in various 2D systems including the amorphous or granular metal ultrathin SC films as well as the recently developed highly crystalline 2D superconductors near the SC critical temperature (T_c) [13–20]. Importantly, this 2D Tinkham's formula assumes that H$_{c2}(\theta)$ is determined by the orbital effect in the entire θ region. On the other hand, Eq. (2) is known as the anisotropic three-dimensional (3D) GL model, which explains H$_{c2}(\theta)$ of anisotropic 3D systems. It is also known that Eq. (2) describes H$_{c2}(\theta)$ of the CeCoIn$_5$ superlattice at low enough temperature ($T \ll T_c$), where H$_{c2}(\theta)$ is governed by the paramagnetic effect in the entire θ regime [3–6]. These situations have been already well established, where the origin of H$_{c2}(\theta)$ has been assumed to be either the orbital effect or the paramagnetic effect in the whole θ regime. In the case of a 2D Ising superconductor, however, the origin of H$_{c2}(\theta)$ should change depending on θ as mentioned above, which does not satisfy the assumptions included in Eqs. (1) and (2). In this paper, we address this issue of how H$_{c2}(\theta)$ behaves in a 2D Ising superconductor which possesses different origins for H$_{c2\parallel}$ and H$_{c2\perp}$.

We prepared NbSe$_2$ ultrathin films, one of the typical 2D Ising superconductors, on insulating sapphire substrates by molecular-beam epitaxy (MBE) [21,22]. Figure 1 shows the temperature (T) dependence of the longitudinal resistance (R) for the different thickness samples, which are normalized by the normal state resistance (R_n) at $T = 8$ K. T_c of the 13 monolayer (13 ML) thick film was 6.2 K, which is close to the bulk value of 7.2 K [23]. Here, T_c was defined as the temperature at $R/R_n = 0.5$. We note that this is the highest T_c that has ever been achieved in NbSe$_2$ thin films grown by MBE or by chemical-vapor deposition [10,24–27]. T_c of the

5-ML-, 2-ML-, and 1-ML-thick films was determined to be 4.8, 3.6, and 2.8 K, respectively. The details of the thin film growth and the transport measurements are described in the Supplemental Material [28].

Figure 2(a) shows the magnetoresistance (MR) isotherms measured with the perpendicular magnetic fields ($\mu_0 H_\perp$; μ_0 is the vacuum permeability) for the 2-ML-thick film, and Fig. 2(b) summarizes the temperature dependence of H$_{c2\perp}$ extracted from the data in Fig. 2(a), which are normalized by the BCS paramagnetic limit H_P. It is clear that H$_{c2\perp}(T)$ stays below H_P in the entire temperature range, indicating that the main contribution to H$_{c2\perp}(T)$ is the orbital effect as mentioned above. This is also confirmed by the linear temperature dependence of H$_{c2\perp}$ [black dashed line in Fig. 2(b)], which is expected if H$_{c2\perp}(T)$ is determined by the orbital effect with the relation

$$\mu_0 \mathrm{H}_{c2\perp}(T) = \frac{\Phi_0}{2\pi\xi(0)^2}(1 - T/T_c), \quad (3)$$

where Φ_0 is the magnetic flux quantum and $\xi(0)$ the GL coherence length at zero temperature. At the other extreme, H$_{c2\perp}(T)$ should follow the square-root behavior if it is determined by the paramagnetic effect [red dashed line in Fig. 2(b)], which is apparently different from the obtained linear temperature dependence. The situation is totally different for the parallel magnetic fields ($\mu_0 H_\parallel$), where H$_{c2\parallel}$ reaches up to 30 T at the lowest temperature as shown in Fig. 2(c). Figure 2(d) summarizes the temperature dependence of H$_{c2\parallel}$ normalized by H_P for the 2-ML- and 1-ML-thick films (red filled symbols) together with those of the exfoliated 2-ML- and 1-ML-thick NbSe$_2$ (blue open symbols) [7]. In general, the orbital limit with the parallel magnetic fields for a 2D superconductor is expressed with the following relation:

$$\mu_0 \mathrm{H}_{c2\parallel}(T) = \frac{\Phi_0\sqrt{12}}{2\pi\xi(0)d_{SC}}\sqrt{1 - T/T_c}. \quad (4)$$

The calculated orbital limit for the 2-ML-thick NbSe$_2$ is far above the experimental data [black dashed line in Fig. 2(d)], indicating that H$_{c2\parallel}(T)$ should be governed by the paramagnetic effect, which is largely enhanced exceeding H_P in almost the entire temperature region. This largely enhanced paramagnetic limit should originate from the unique Ising pairing as previously discussed in NbSe$_2$ ultrathin films [7,10]. In fact, our data agree quite well with the previous results of the exfoliated NbSe$_2$ flakes, indicating that our MBE-grown NbSe$_2$ ultrathin films could be regarded as 2D Ising superconductors as well. In any case, these MR measurements verified that H$_{c2\perp}(T)$ is determined by the orbital effect while H$_{c2\parallel}(T)$ is governed by the paramagnetic effect in almost all the temperature regime in the present system, which is unique to 2D Ising superconductors distinct from other systems. We note that the 1-ML-thick NbSe$_2$ also satisfies this condition (see Supplemental Material [28] for the details).

The angle dependence of H$_{c2}$ indeed unveiled the unique aspect of a 2D Ising superconductor. Figure 3(a) shows the set of the MR data of the 2-ML-thick film at the lowest temperature $T = 0.9$ K ($T/T_c = 0.24$) with the different field angle, and Fig. 3(b) summarizes the angle dependence of H$_{c2}$. The black line represents H$_{c2}(\theta)$ calculated based on Eq. (1)
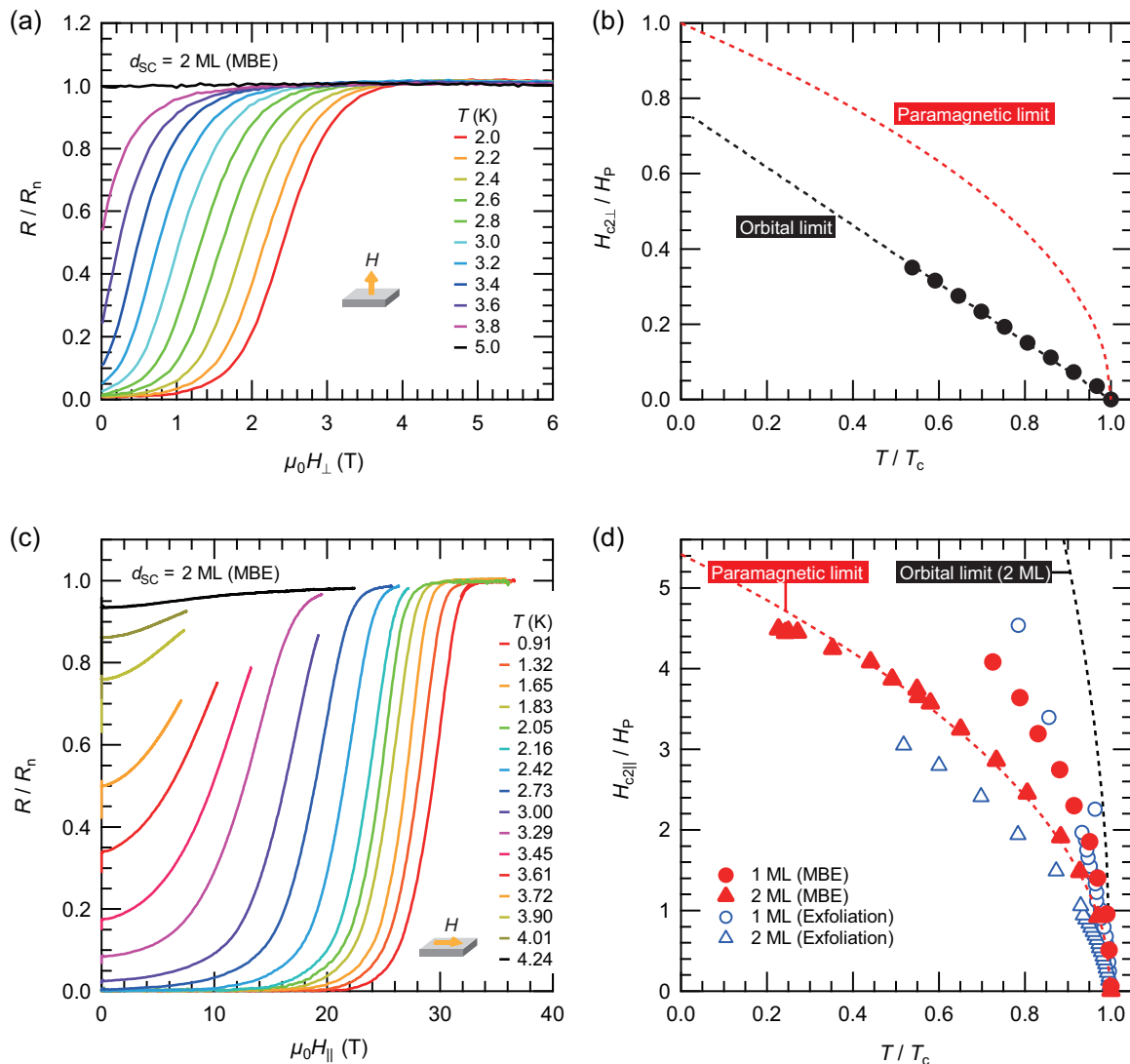
FIG. 2. The H$_{c2}$ measurements of the 2-ML-thick NbSe$_2$ film with the perpendicular ($\mu_0H_\perp$) and parallel ($\mu_0H_\parallel$) magnetic fields. (a) The normalized MR isotherms with $\mu_0H_\perp$. (b) H$_{c2\perp}$ versus T normalized by H_P and T_c, respectively. The black dashed line is the linear fit with Eq. (3) to the experimental data, providing $\xi(0) = 7.85$ nm. The red dashed line corresponds to the behavior expected when H$_{c2\perp}$ is limited by the paramagnetic effect with the relation H$_{c2\perp} = H_P(1-T/T_c)^{1/2}$. (c) The normalized MR isotherms of the same sample with $\mu_0H_\parallel$. (d) H$_{c2\parallel}$ versus T normalized by H_P and T_c, respectively. The black dashed line corresponds to the behavior expected when H$_{c2\parallel}$ is governed by the orbital effect calculated with $\xi(0) = 7.85$ nm and $d_{SC} = 2$ ML based on Eq. (4). The red dashed line is the fit to the experimental data assuming the paramagnetic limit. The H$_{c2\parallel}/H_P$ versus T/T_c of the exfoliated NbSe$_2$ flakes are also shown by open blue symbols.

(the 2D Tinkham's formula) assuming that H$_{c2}(\theta)$ is limited by the pure orbital effect. It is clear that the experimental data largely deviated from the calculated black line around $\theta = 90°$, which is consistent with the above discussion that H$_{c2\parallel}$ is dominated by the paramagnetic effect in the present case. On the other hand, the blue line shows H$_{c2}(\theta)$ calculated based on Eq. (2) that describes H$_{c2}(\theta)$ limited by the pure paramagnetic effect, which also fails to reproduce the experimental data around $\theta = 90°$. In fact, the observed H$_{c2}(\theta)$ shows the cusplike behavior around $\theta = 90°$ as if it is determined by the 2D orbital effect. This is very surprising and intriguing given that H$_{c2\parallel}$ is governed by the paramagnetic effect in the present case, in marked contrast to the case of the CeCoIn$_5$ superlattice. The striking difference between the

2D Ising superconductors including NbSe$_2$ ultrathin films and the CeCoIn$_5$ superlattice is the origin of H$_{c2\perp}$; it is limited by the paramagnetic effect in the CeCoIn$_5$ superlattice at $T \ll T_c$ [3–6], whereas it is determined by the orbital effect in the NbSe$_2$ ultrathin films at all the temperatures. Therefore, in order to describe H$_{c2}(\theta)$ of the NbSe$_2$ ultrathin films [and more generally H$_{c2}(\theta)$ of all the 2D Ising superconductors], the crossover between the orbital effect and the paramagnetic effect with varying θ should be considered. However, those two origins of H$_{c2}$ have been separately discussed so far, for at least at the fixed temperature, and connection of these two origins in one formalism is required.

Here we propose the phenomenology of H$_{c2}(\theta)$, where both the orbital and paramagnetic effects are considered. The
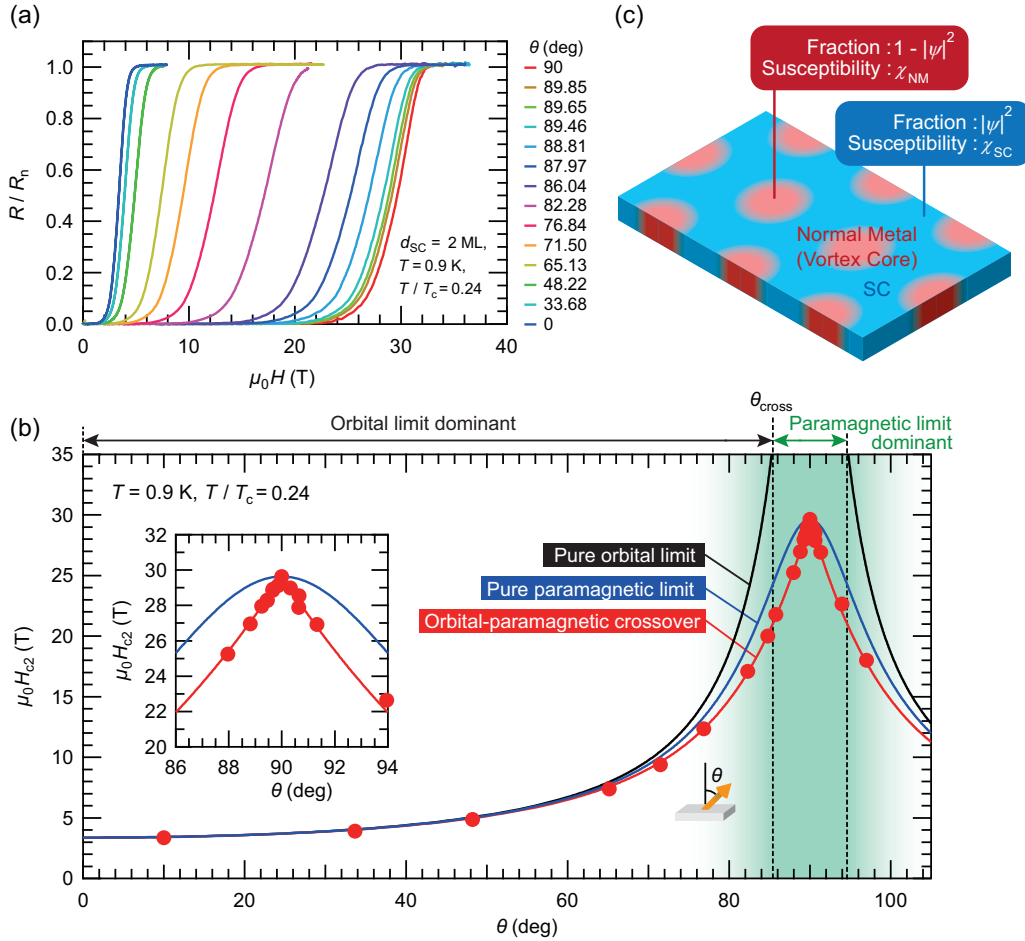
FIG. 3. The angle dependence of H$_{c2}$ of the 2-ML-thick NbSe$_2$ film at $T = 0.9$ K ($T/T_c = 0.24$). (a) The normalized MR data with the different field angle θ. (b) H$_{c2}$ versus θ. The black line shows H$_{c2}$ (θ) calculated based on Eq. (1) using $\xi(0) = 7.85$ nm and $d_{SC} = 2$ ML, which assumes that H$_{c2}$ is limited by the pure orbital effect in the entire θ regime. The blue line represents H$_{c2}(\theta)$ calculated based on Eq. (2) using the experimentally obtained H$_{c2\parallel}$, which assumes that H$_{c2}$ is limited by the pure paramagnetic effect in the entire θ regime. The red line demonstrates H$_{c2}(\theta)$ calculated based on Eq. (9) with $x = 0.92$, which corresponds to $\frac{H_{c2\perp, \text{ orbital}}}{H_{c2\perp, \text{ para}}} = 0.3$. θ_{cross} is the crossover angle defined such that the first and second terms in Eq. (9) are equal. The inset shows the magnified plot around $\theta = 90°$. (c) A schematic of a proposed model, where the contribution from the paramagnetic effect to H$_{c2}$ is considered through the space dependent spin susceptibility originating from the NM region (i.e., vortex core) and the SC region.

free energy of the orbital effect F_{orbital} is described by the standard GL model [29],

$$F_{\text{orbital}} = \int d\boldsymbol{r} \left[-a|\psi|^2 + \frac{b}{2}|\psi|^4 + \frac{\hbar^2}{2m^*}\left| \left(\nabla - \frac{i2e}{\hbar}\boldsymbol{A} \right)\psi \right|^2 \right],$$
(5)

where $a = \hbar^2/[2m^*\xi(0)^2]$ and b are the phenomenological parameters, m^* the effective mass of an electron pair, ψ the complex order parameter, e the charge of electron, and $\hbar$ the reduced Planck constant, respectively. From the solution of Eq. (5), the orbital effect represented by the vortex picture is obtained, which results in the 2D Tinkham's formula of Eq. (1) at the 2D limit [13]. On the other hand, the free energy of the paramagnetic effect F_{para} is obtained from the free energy of paramagnetism as follows:

$$F_{\text{para}} = -\tfrac{1}{2}\boldsymbol{B} \cdot \boldsymbol{H}. \tag{6}$$

In the case of the pure paramagnetic limit, we simply consider the free energy of the uniform SC order parameter ψ. In contrast, when both the orbital and paramagnetic effects are considered, the free energy is described with the space dependent ψ. Here we consider the situation where both the normal metallic (NM) and SC regions are coexisting with the fraction of $1 - |\psi|^2$ and $|\psi|^2$, which is characterized with the spin susceptibility χ_{NM} and χ_{SC}, respectively, as shown in Fig. 3(c). Then, the free energy in Eq. (6) can be rewritten as

$$F_{\text{para}} = -\frac{1}{2} \int d\boldsymbol{r}[(1 - |\psi|^2)\boldsymbol{B}_{\text{NM}} \cdot \boldsymbol{H} + |\psi|^2\boldsymbol{B}_{\text{SC}} \cdot \boldsymbol{H}], \quad (7)$$

where $\boldsymbol{B}_{\text{NM}}$ and $\boldsymbol{B}_{\text{SC}}$ are the magnetic flux densities in the NM and SC regions, respectively. Now, we consider the total free energy F_{total} as

$$F_{\text{total}} = F_{\text{orbital}} + F_{\text{para}}. \tag{8}$$

From Eq. (8), we can derive H$_{c2}(\theta)$ including contributions both from the orbital and paramagnetic effects. When the paramagnetic effect is dominant for H$_{c2\parallel}$, H$_{c2}(\theta)$ should follow

$$x\left|\frac{H_{c2}(\theta)\cos\theta}{H_{c2\perp}}\right| + (1-x)\left[\frac{H_{c2}(\theta)\cos\theta}{H_{c2\perp}}\right]^2$$
$$+ \left[\frac{H_{c2}(\theta)\sin\theta}{H_{c2\parallel}}\right]^2 = 1, \qquad (9)$$

where $x : (1-x)$ satisfies the relation

$$x : (1-x) = 1 : \frac{1}{2}\left\{\sqrt{1 + 4\left(\frac{H_{c2\perp,\ orbital}}{H_{c2\perp,\ para}}\right)^2} - 1\right\}, \quad (10)$$

and H$_{c2\perp,\ orbital}$ (H$_{c2\perp,\ para}$) corresponds to the orbital (paramagnetic) limit for the perpendicular magnetic fields. The details of the formalism are written in the Supplemental Material [28].

Now, H$_{c2}(\theta)$ can be derived from Eq. (9) even when the orbital and paramagnetic effects both contribute to H$_{c2\perp}$, and importantly, the value x provides the ratio of the contribution from the orbital and paramagnetic effects to H$_{c2\perp}$. When H$_{c2\perp}$ is dominated by the paramagnetic effect (H$_{c2\perp,\ para} \ll$ H$_{c2\perp,\ orbital}$), x approaches 0 and Eq. (9) becomes Eq. (2). This is the case for the CeCoIn$_5$ superlattice at $T \ll T_c$, where H$_{c2}(\theta)$ is well fitted by Eq. (9) with $x \sim 0$ [3–6]. On the contrary, when H$_{c2\perp}$ is governed by the orbital effect (H$_{c2\perp,\ para} \gg$ H$_{c2\perp,\ orbital}$), x approaches 1 and Eq. (9) matches Eq. (1). In the present case, H$_{c2}(\theta)$ could be well fitted by Eq. (9) with $x = 0.92$ as shown by the red line in Fig. 3(b), suggesting that H$_{c2\perp}$ of our 2-ML-thick NbSe$_2$ is mainly limited by the orbital effect. However, very interestingly, the obtained x turned out to be much larger than 0.72, implying that the paramagnetic limit should be enhanced by more than twice even for the perpendicular magnetic fields (see Supplemental Material [28] for the details). The resultant cusplike behavior around $\theta = 90°$ even in the paramagnetic-limit-dominant regime implies that the vortices are introduced once the field angle is slightly deviated from $\theta = 90°$. In addition, H$_{c2}(\theta)$ demonstrates smooth variation from H$_{c2\perp}$ to H$_{c2\parallel}$, indicating the crossover behavior from the pure orbital-limited regime at $\theta = 0°$ to the pure paramagnetic-limited regime at $\theta = 90°$ with the crossover angle θ_{cross} of about 86°, which is defined such that the first and third terms in Eq. (9) are equal. This crossover behavior between the orbital and paramagnetic limits could be attributed to the continuous shift of the energy of the wave function in the harmonic oscillator potential induced by the paramagnetic effect (see Supplemental Material [28] for the details). Figure 4 summarizes H$_{c2}(\theta)$ taken at different temperatures, $T/T_c = 0.24$, 0.54, and 0.96, showing similar cusplike behavior at all the temperatures that could be nicely fitted by Eq. (9) with $x \sim 1$. This is reasonable considering that H$_{c2\perp}$ and H$_{c2\parallel}$ are dominated by the orbital and paramagnetic effects at the entire temperature regime in this system, indicating that the cusplike behavior should be intrinsic to 2D Ising superconductors.
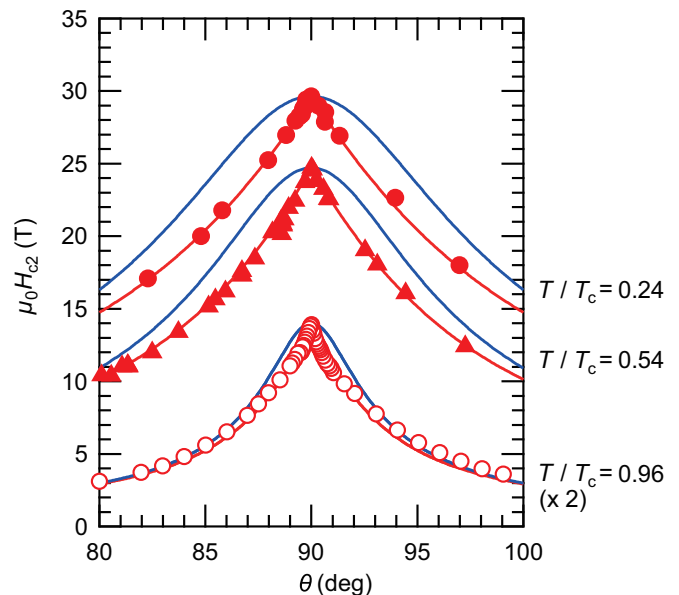
FIG. 4. H$_{c2}(\theta)$ of the 2-ML-thick NbSe$_2$ film at $T/T_c = 0.24$, 0.54, and 0.96 around $\theta = 90°$. The blue and red lines correspond to H$_{c2}(\theta)$ calculated based on Eq. (2) or based on Eq. (9) with $x \sim 1$, respectively.

In conclusion, we investigated the angle dependence of H$_{c2}$ in a 2D Ising superconductor NbSe$_2$ ultrathin film, and revealed that it exhibits cusplike behavior around the parallel magnetic fields even at the lowest temperature $T/T_c = 0.24$ where H$_{c2\parallel}$ should be dominated by the paramagnetic effect. We derived a phenomenological formula that describes H$_{c2}(\theta)$ in this unique system, and successfully reproduced the experimental data. The present results suggest that the cusplike behavior in H$_{c2}(\theta)$ around the parallel fields captures the essential feature of 2D Ising superconductors, which should originate from the fact that H$_{c2\perp}$ is determined by the orbital effect with the enhanced paramagnetic limit. We emphasize that the proposed model enables us to estimate the contribution from the paramagnetic effect even if H$_{c2}$ is primarily governed by the orbital effect, offering a powerful approach for comprehensive understanding of the origin of H$_{c2}$.

[1] P. A. Frigeri, D. F. Agterberg, A. Koga, and M. Sigrist, Phys. Rev. Lett. **92**, 097001 (2004).

[2] E. Bauer, G. Hilscher, H. Michor, C. Paul, E. W. Scheidt, A. Gribanov, Y. Seropegin, H. Noël, M. Sigrist, and P. Rogl, Phys. Rev. Lett. **92**, 027003 (2004).

[3] Y. Mizukami, H. Shishido, T. Shibauchi, M. Shimozawa, S. Yasumoto, D. Watanabe, M. Yamashita, H. Ikeda, T. Terashima, H. Kontani, and Y. Matsuda, Nat. Phys. **7**, 849 (2011).

[4] S. K. Goh, Y. Mizukami, H. Shishido, D. Watanabe, S. Yasumoto, M. Shimozawa, M. Yamashita, T. Terashima, Y. Yanase, T. Shibauchi, A. I. Buzdin, and Y. Matsuda, Phys. Rev. Lett. **109**, 157006 (2012).

[5] M. Shimozawa, S. K. Goh, R. Endo, R. Kobayashi, T. Watashige, Y. Mizukami, H. Ikeda, H. Shishido, Y. Yanase, T. Terashima, T. Shibauchi, and Y. Matsuda, Phys. Rev. Lett. **112**, 156404 (2014).

[6] M. Naritsuka, T. Ishii, S. Miyake, Y. Tokiwa, R. Toda, M. Shimozawa, T. Terashima, T. Shibauchi, Y. Matsuda, and Y. Kasahara, Phys. Rev. B **96**, 174512 (2017).

[7] X. Xi, Z. Wang, W. Zhao, J. H. Park, K. T. Law, H. Berger, L. Forró, J. Shan, and K. F. Mak, Nat. Phys. **12**, 139 (2016).

[8] J. M. Lu, O. Zheliuk, I. Leermakers, N. F. Q. Yuan, U. Zeitler, K. T. Law, and J. T. Ye, Science **350**, 1353 (2015).

[9] Y. Saito, Y. Nakamura, M. S. Bahramy, Y. Kohama, J. Ye, Y. Kasahara, Y. Nakagawa, M. Onga, M. Tokunaga, T. Nojima, Y. Yanase, and Y. Iwasa, Nat. Phys. **12**, 144 (2016).

[10] Y. Xing, K. Zhao, P. Shan, F. Zheng, Y. Zhang, H. Fu, Y. Liu, M. Tian, C. Xi, H. Liu, J. Feng, X. Lin, S. Ji, X. Chen, Q. K. Xue, and J. Wang, Nano Lett. **17**, 6802 (2017).

[11] E. Navarro-Moratalla, J. O. Island, S. Manãs-Valero, E. Pinilla-Cienfuegos, A. Castellanos-Gomez, J. Quereda, G. Rubio-Bollinger, L. Chirolli, J. A. Silva-Guillén, N. Agraït, G. A. Steele, F. Guinea, H. S. J. Van Der Zant, and E. Coronado, Nat. Commun. **7**, 11043 (2016).

[12] E. Sohn, X. Xi, W. He, S. Jiang, Z. Wang, K. Kang, J. Park, H. Berger, L. Forró, K. T. Law, J. Shan, and K. F. Mak, Nat. Mater. **17**, 504 (2018).

[13] M. Tinkham, Phys. Rev. **129**, 2413 (1963).

[14] F. E. Harper and M. Tinkham, Phys. Rev. **172**, 441 (1968).

[15] A. P. Petrović, A. Paré, T. R. Paudel, K. Lee, S. Holmes, C. H. W. Barnes, A. David, T. Wu, E. Y. Tsymbal, and C. Panagopoulos, New J. Phys. **16**, 103012 (2014).

[16] K. Ueno, T. Nojima, S. Yonezawa, M. Kawasaki, Y. Iwasa, and Y. Maeno, Phys. Rev. B **89**, 020508(R) (2014).

[17] Y. Saito, Y. Kasahara, J. Ye, Y. Iwasa, and T. Nojima, Science **350**, 409 (2015).

[18] C. Xu, L. Wang, Z. Liu, L. Chen, J. Guo, N. Kang, X.-L. Ma, H.-M. Cheng, and W. Ren, Nat. Mater. **14**, 1135 (2015).

[19] H. Nam, H. Chen, T. Liu, J. Kim, C. Zhang, J. Yong, T. R. Lemberger, P. A. Kratz, J. R. Kirtley, K. Moler, P. W. Adams, A. H. MacDonald, and C.-K. Shih, Proc. Natl. Acad. Sci. USA **113**, 10513 (2016).

[20] A. M. R. V. L. Monteiro, D. J. Groenendijk, I. Groen, J. De Bruijckere, R. Gaudenzi, H. S. J. van der Zant, and A. D. Caviglia, Phys. Rev. B **96**, 020504(R) (2017).

[21] M. Nakano, Y. Wang, Y. Kashiwabara, H. Matsuoka, and Y. Iwasa, Nano Lett. **17**, 5595 (2017).

[22] Y. Wang, M. Nakano, Y. Kashiwabara, H. Matsuoka, and Y. Iwasa, Appl. Phys. Lett. **113**, 073101 (2018).

[23] H. A. Leupold, F. Rothwarf, J. J. Winter, J. T. Breslin, R. L. Ross, T. R. AuCoin, and L. W. Dubeck, J. Appl. Phys. **45**, 5399 (1974).

[24] M. M. Ugeda, A. J. Bradley, Y. Zhang, S. Onishi, Y. Chen, W. Ruan, C. Ojeda-Aristizabal, H. Ryu, M. T. Edmonds, H. Z. Tsai, A. Riss, S. K. Mo, D. Lee, A. Zettl, Z. Hussain, Z. X. Shen, and M. F. Crommie, Nat. Phys. **12**, 92 (2016).

[25] H. Wang, X. Huang, J. Lin, J. Cui, Y. Chen, C. Zhu, F. Liu, Q. Zeng, J. Zhou, P. Yu, X. Wang, H. He, S. H. Tsang, W. Gao, K. Suenaga, F. Ma, C. Yang, L. Lu, T. Yu, E. H. T. Teo, G. Liu, and Z. Liu, Nat. Commun. **8**, 394 (2017).

[26] Y. Nakata, K. Sugawara, S. Ichinokura, Y. Okada, T. Hitosugi, T. Koretsune, K. Ueno, S. Hasegawa, T. Takahashi, and T. Sato, npj 2D Mater. Appl. **2**, 12 (2018).

[27] H. Lin, Q. Zhu, D. Shu, D. Lin, J. Xu, X. Huang, W. Shi, X. Xi, J. Wang, and L. Gao, Nat. Mater. **18**, 602 (2019).

[28] See Supplemental Material at http://link.aps.org/supplemental/10.1103/PhysRevResearch.2.012064 for details of the thin film growth and the H_{c2} measurements, as well as the details of the formalism and further discussions.

[29] M. Tinkham, *Introduction to Superconductivity*, 2nd ed. (McGraw-Hill, New York, 1996).